



Volatile fatty acid augmentation and microbial community responses in anaerobic co-fermentation process of waste-activated sludge mixed with corn stalk and livestock manure

Xiaodong Xin¹ · Junguo He¹ · Wei Qiu^{1,2}

Received: 9 May 2017 / Accepted: 23 November 2017 / Published online: 3 December 2017
© Springer-Verlag GmbH Germany, part of Springer Nature 2017

Abstract

This study investigated the acidogenic and microbiological perspectives in the anaerobic co-fermentation of waste-activated sludge (WAS) mixed with corn stalk (CS) and pig manure (PM). The volatile fatty acids (VFAs) increased dramatically to over 5000 mg COD/L accumulation just within 4–5 days with the feedstock carbon to nitrogen (C/N) ratio regulation of 20/1. The CS and PM addition enhanced the compressibility of fermentation residuals by increasing the particle distribution spread index (DSI). Moreover, the external carbon addition conducted to bacterial consortia diversity rising and uneven population distribution in the co-fermentation, which contributed to VFAs accumulation potentially. The organic loading rate (OLR) correlated with bacterial community closely at the early stage (days 1–5), while the oxidation-reduction potential (ORP) and pH played more important roles on bacterial consortia at the terminal stage (days 6–10). The C/N ratio adjustment by CS and PM and proper optimizations of OLR, pH, and ORP at various running stages facilitated VFA accumulation during the co-fermentation operation.

Keywords Waste-activated sludge · Anaerobic co-fermentation · Corn stalk and pig manure · VFAs accumulation · Bacterial community · Diversity · Redundancy analysis

Introduction

Last decade, the waste-activated sludge (WAS) was produced dramatically from the wastewater treatment plants (WWTPs) as the fast urbanization in China (Dai et al. 2016). From 2007 to 2013, the total sludge production in China rose significantly with an annual growth of 13% (Yang et al. 2015). Meanwhile, China is one of the largest countries with remarkable agricul-

ture and livestock wastes generation in the world. The production of crop residues (such as the corn stalk, CS) was estimated at 600–800 million tonnes per year, causing severe hazes pollution by the traditional incineration treatment (Jiang et al. 2012). Besides, the livestock waste (like pig manure, PM) presented a rising production resulting in inevitable environmental contaminations in China due to its serious pathogenicity and pollution on soil, water, and air, although it contained plenty of high-concentration biodegradable nutrients (Zheng et al. 2015).

On the other hand, the anaerobic fermentation was considered as an effective option for organic waste reduction with obtaining valuable intermediate products, such as volatile fatty acids (VFAs), which could be used (1) as the external carbon resource in biological nutrient removal processes (Li et al. 2011), (2) for electricity generation by microbiological fuel cells (MFCs) (Chen et al. 2013), and (3) for polyhydroxyalkanoate (PHA) synthesis (Jiang et al. 2009). Thus, the WAS anaerobic fermentation treatment had attracted wide attention and deep investigations previously (Jiang et al. 2009; Li et al. 2011). However, its drawbacks could not be neglected, such as low organic

Responsible editor: Gerald Thouand

Electronic supplementary material The online version of this article (<https://doi.org/10.1007/s11356-017-0834-0>) contains supplementary material, which is available to authorized users.

✉ Wei Qiu
qiuweihi@126.com

¹ School of Municipal and Environmental Engineering, Harbin Institute of Technology (HIT), Harbin 150090, China

² State Key Laboratory of Urban Water Resource and Environment, Harbin Institute of Technology (SKLUWRE, HIT), Harbin 150090, China

conversion efficiency, long retention time, and low fermentation efficiency (Dai et al. 2016). Moreover, the carbon-to-nitrogen mass ratio (C/N) of feedstock played an essential role on the performance of anaerobic biochemical processes. The excess ammonium in the feedstock limited the microbial biochemical processes and constrained VFAs' further accumulation in the anaerobic fermentation significantly (Nielsen and Angelidaki 2008). Feng et al.'s study reported that the low C/N ratio of WAS restricted the VFA (especially the propionate) generation during the fermentation process, and a balancing C/N ratio by adding carbohydrates favored VFA accumulation remarkably (Feng et al. 2009). Faced up to such a situation, researchers proposed that the theoretical C/N value of 20/1 was able to bring about a maximal VFA accumulation yield in WAS anaerobic fermentation by external carbon source addition (Jia et al. 2013; Luo et al. 2014). Thus, the anaerobic co-fermentation of WAS with other organic substances got to be a key approach to conquer the disadvantages caused by the carbon source shortage (low C/N ratio). However, most of the current literatures paid much attention on facilitating VFA production in WAS co-fermentation with food wastes (fat, oil, and grease) (Alqaralleh 2016; Jang et al. 2016; Ziels et al. 2016) or adding promoters (like CaO_2) (Li et al. 2015). Scarce studies focused on VFA accumulation in the WAS co-fermentation by adding the CS and livestock wastes (such as PM) (Lu et al. 2010). Additionally, plenty of pretreatments were implemented for prompting WAS anaerobic fermentation performance as the rate-limiting step of feedstock solubilization determined the total co-fermentation efficiency. Therefore, the physical (Salsabil et al. 2009; Barber 2016; Lo et al. 2016), chemical (Li et al. 2011; Mahdad et al. 2016), and biological methods (Teo and Wong 2014; Xin et al., 2017) were adopted widely for increasing the anaerobic fermentation performance previously. Among them, the biological enzymolysis presented its superiority, exhibiting high WAS solubilization efficiency within a brief operation time (just 3–4 h) (Yang et al. 2010; Xin et al. 2016).

Microbial community structure and dynamics (including diversity and distributive evenness) were related to system performance stability closely (Loreau et al. 2001; Wittebolle et al. 2009). The key basis of VFA stable accumulation was the establishment of a microbial community delicately balanced between the bacteria and archaea in anaerobic fermentation process (Jang et al. 2016). The fermentation process imbalance resulted in the malfunctioning of microbial community by adverse environmental variables (Guo et al. 2014). Moreover, the organic loading rate (OLR), oxidation-reduction potential (ORP), and pH were the important impact factors, which were responsible for the balance of microbial community between bacteria and archaea in the fermentation process (Chen et al. 2015; Jang et al. 2016). Thus, revealing the relationship of microbial community structure and dynamics with impact factors would better reveal the microbial ecology during the fermentation

process, which was conducive to optimize operations for facilitating further VFA accumulation.

The main objective of this study was to disclose the VFA accumulation performance and microbial community responses in WAS anaerobic co-fermentation process mixed with CS and PM. The detailed aims were to (1) illustrate the enhanced VFA accumulation performance in the co-fermentation process of WAS, CS, and PM; (2) reveal the relationship of bacterial community dynamic behaviors (evolutions, diversity, and evenness changes) with VFA accumulation in the co-fermentation system; and (3) elucidate the correlation of bacterial community composition with the co-fermentation impact factors, which was conducive to optimize the co-fermentation operations.

Materials and methods

WAS, CS, and PM pretreatments

The WAS used in this study was taken from the secondary sedimentation tank of a full-scale municipal wastewater treatment plant in Harbin, China. Its detailed traits were as follows: total suspended solids (TSS) $14,560 \pm 165$ mg/L, volatile suspended solids (VSS) $10,780 \pm 115$ mg/L, and pH value 6.8 ± 0.1 . WAS was pretreated by a blend of hydrolytic commercial enzymes (comprising lysozyme, α -amylases, protease, and cellulose with corresponding enzymatic activities of 20,000, 6000, 60,000, and 30 U/mg, respectively) for 4 h within a water bath at 37 ± 1 °C. The proportion of individual enzyme in the mixture was maintained at 1:1:1:1 (mass ratio) with the adding dosage of 5% (enzymes weight/TSS, w/w). The mass ratio of mixture 1:1:1:1 and the enzyme weight/TSS ratio of 5% were selected by evaluating the operational protocol of previous studies. In Yang et al.'s study, the mixing ratio 1:1 of enzyme blend (protease and amylase) led to high WAS hydrolysis efficiency. The enzyme mixture adding dosages of 3, 6, 12, and 18% for boosting WAS hydrolysis were investigated comprehensively, stating that 6% appeared to be the optimum dosage in terms of economy and efficiency (Yang et al. 2010). In Parmar et al.'s study, the mixing ratio of 1:1:1 was adopted by weight of enzyme blend (cellulase, protease and lipase), which was used to pre-hydrolyze WAS for detecting the solids volume reduction and settlement property changes (Parmar et al. 2001). In Yu et al.'s study, the identical individual enzyme adding dosage (15 mL protease solution and 15 mL amylase solution) was adopted in the study (Yu et al. 2013). Furthermore, the WAS solubilization caused by the mass ratio 1:1:1:1 of enzyme mixture (lysozyme, α -amylases, protease and cellulose) and 5% adding dosage (enzymes weight/TSS) was investigated in detail previously in a previous study (Xin et al. 2016). Thus, the individual enzyme adding ratio of 1:1:1:1

Table 1 Element proportions of different substrates

	C (%)	N (%)	C/N ratio
CS	43.58 ± 0.08	0.31 ± 0.11	151.34 ± 52.75
PM	42.39 ± 0.23	3.96 ± 0.01	10.70 ± 0.08
WAS	57.01 ± 0.35	6.26 ± 0.21	9.10 ± 0.55

in the enzyme blend and the enzyme weight/TSS ratio of 5% were adopted in this study.

The CS was taken from the rural land in the suburb of Harbin City (China) after the agriculture harvest. The PM was obtained from a pig farm near Harbin City. Both the CS and PM were baked at 105 °C for 12 h (drying CS and PM for the grinding process easily) prior to the co-fermentation. Subsequently, the CS and PM were smashed by using a Chinese medicine grinder and then filtrated by a 40-mesh sieve (450 µm diameter). The CS and PM powders were treated by high-pressure steam for 1 h at 121 °C and then soaked by 1 M NaOH (100 mL) for 24 h for promoting their biodegradability. The detailed C and N element proportions of CS, PM and WAS were listed in Table 1.

Anaerobic fermentation device and experiment

Four cylindrical anaerobic bioreactors were designed to be used for WAS fermentation in this study, which were made of a polymethyl methacrylate according to a previous study (Xin et al., 2017). The effective reaction volume of each was 2 L with 20 cm height (height to diameter ratio was 2:1). A blender was installed at the top of the reactor to stir the fermentation organic matters properly. The interface was blocked by a water seal unit on the reactor to keep a strict anaerobic state (dissolved oxygen was less than 0.1 mg/L). The reactor contained a fermentation cylinder with an annular water bath area (around the fermentation cylinder for keeping a constant fermentation temperature). The operational temperature was maintained at 35 ± 1 °C by the water circulation powered by a mini pump and a water heater. The stirring speed was kept at 60 r/min constantly. N₂ was used to be injected into each bioreactor to expel the oxygen mostly. The anaerobic

fermentation reactor was operated in batch-feeding model. The fermentation samples were obtained regularly from the sampling port of the reactor, which were used for experimental detection and analysis.

Four batch anaerobic fermentation experiments were operated simultaneously for 10 days fed with the various substrates with different C/N ratios (listed in Table 2). When one batch fermentation test was accomplished, the corresponding duplicate fermentation experiments were conducted subsequently.

Analytical methods

The soluble COD (SCOD), TSS, and VSS of the collected samples were detected in accordance with standard methods (APHA, 1998). Soluble protein was detected by a modified BCA kit (Sangon, China). Soluble carbohydrate was measured by the phenol-sulfuric acid method with glucose as the standard (Michel et al. 1956). The concentration and composition of VFAs were determined by an Agilent 6890 gas chromatography (GC) with flame ionization detector and DBWAXTRE column (30 m × 0.32 mm × 0.25 mm), which was operated according to a previous literature (Yan et al. 2010). The biogas composition was detected by using a GC (SP-6801 T, China) according to a previous literature (Chen et al. 2015). Morphological properties of the fermentative sludge samples were illustrated by particle size distribution and distribution spread index (DSI) of sludge flocs. Particle size distribution was determined using a laser diffraction sensor (Mastersizer 2000, Malvern Firm). Characteristics of soluble organics in solution of fermentative WAS were assessed by excitation-emission matrix (EEM) spectra (FP6500, JASCO, Japan), which could grasp corresponding scanning emission spectra from 220 to 650 nm at 2-nm increments by changing the excitation wavelength from 220 to 500 nm at 5-nm sampling intervals. Oxidation-reduction potential (ORP) of the fermentative sludge was detected by using ORP measuring instrument (Hanna, Italy). The pH was detected by the pH measuring instrument (Hanna, Italy). The elemental composition, such as C and N of the feedstock, was analyzed by a Vario EL/microcube elemental analyzer (Elementar,

Table 2 The feed compositions in the anaerobic fermentation/co-fermentation process

	WAS	CS	PM	C/N ratio
Fermentation process 1	1 L (pretreated by enzymolysis)	31 g (pretreated)	5 g (pretreated)	20/1
Fermentation process 2	1 L (pretreated by enzymolysis)	25.5 g (pretreated)	–	20/1
Fermentation process 3	1 L (pretreated by enzymolysis)	–	–	9/1
Fermentation process 4 (control experiment)	1 L (fresh WAS)	–	–	9/1

– no addition

Germany). All the experimental data were expressed as the average value ± standard deviation format.

Microbial community analysis

Terminal restriction fragment length polymorphism (T-RFLP) was used to monitor microbial community dynamics. The detailed steps were as follows:

1. Genomic DNA was extracted from the sludge sample and the corresponding parallel sample (about 5 mL), respectively (Power Soil DNA Isolation Kit, Sangon of China) and then mixed them together.
2. Polymerase chain reaction (PCR) and product recovery. Common primers of former primer 8F (5'- AGAGTTTG ATCCTGCCTCAG-3'), labeled by FAM fluorescent sign and reverse primer 1492R (5'-GGTTACCTTGTTAC GACTT-3') (Sangon, China) were used to amplify the bacterial 16S rDNA sequence (Turner et al. 1999). The PCR system was as follows: 10 × PCR buffer (Sangon, China) 5 μL, dNTP (Sangon, China) 4 μL, DNA polymerase (TransGen, China) 1 μL, template DNA (Genomic DNA) 1 μL, former primer 1 μL, reverse primer 1 μL, sterile water 37 μL. The total volume was 50 μL. The PCR process was: 4 min at 99 °C followed by 30 cycles of 30 s at 94 °C, 30 s at 55 °C, and 30 s at 72 °C, followed by 8-min final extension at 72 °C.
3. Restriction endonuclease digestion.
4. Capillary electrophoresis to gain the T-RF information. The obvious T-RFs smaller than 50 bp or larger than 600 bp were excluded from the analysis. Peaks with an area less than 1% were not considered in the results due to the issue of accuracy degree of the ABI PRISM 3130 genetic analyzer. The bacterial phylogenetic assignment was performed using a default database generated from MiCA (<http://mica.ibest.uidaho.edu/>) and default fragment bin tolerance window setting.

Data analysis

DSI was used to evaluate the sludge filtration characteristics and could be calculated as follows (Mohamed 2008):

$$DSI = \frac{d_{90} - d_{10}}{2 \times d_{50}} \quad (1)$$

where d_{90} was the diameter corresponding to 90% of cumulative undersize, d_{50} was the median diameter, and d_{10} stood for the diameter corresponding to 10% of cumulative undersize.

Shannon index (H) was used widely to evaluate the community diversity (Saikaly et al. 2005):

$$H = -\sum p_i \ln p_i \quad (i = 1, 2, \dots, S) \quad (2)$$

where p_i stood for the relative abundance of the species i (the peak area of each T-RF from species i /total areas of all T-RFs); S was the number of the total T-RFs. The index ranged from 0 (no common T-RF) to 1.0 (identical T-RF patterns).

Pareto-Lorenz curve (PL curve) was used to describe the microbial community distributive evenness (Marzorati et al. 2008), which was associated with the system performance closely (Wittebolle et al. 2009). The vertical axis within it represented the cumulative proportion of OTU abundance, and the abscissa axis stood for the cumulative proportion of OTUs. The 45° diagonal represented the perfect evenness of a community. PL curve deviating from the 45° diagonal line indicated the uneven species distribution in the community.

Statistical analysis

The redundancy analysis (RDA) based on the microbial community composition and fermentation impact factors of pH, ORP, and OLR were performed by using CANOCO 4.5 software. The Monte Carlo test was performed with 500 permutations of forward selection to the RDA analysis, respectively (Morowitz et al. 2011). Explanatory variables that contributed significant improvement ($P < 0.05$) to the explanatory power of the RDA models were indicated by red arrows in the ordinations, and the T-RFs were presented by blue arrows.

Results and discussion

The mass balance on WAS solubilization by enzymolysis pretreatment

In order to evaluate the correlation between VSS reduction with the soluble substance (SCOD) increase by the enzymolysis pretreatment, a mass balance on WAS solubilization has been established in Fig. 1. It could be seen that after the enzymatic pretreatment, the SCOD increased dramatically from the initial 238.4 to 5585.6 mg/L (5.35 g/L augmentation roughly) in the liquid phase of WAS, whereas the VSS presented a clear decrease of 3.80 g/L (from 10.78 to 6.98 g/L) in the solid phase. Based upon the theoretical relationship of 1.42 g COD per g VSS (represented by $C_5H_7NO_2$) (Bruce

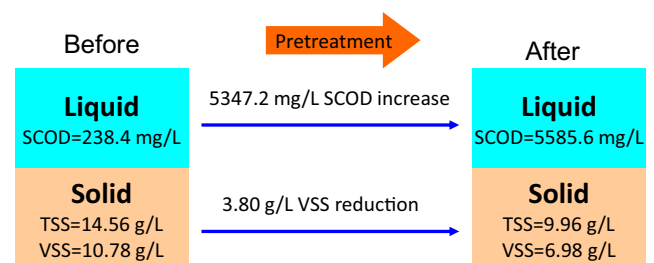


Fig. 1 Mass balance on the waste-activated sludge by the enzymolysis pretreatment in this study

and Perry, 2001; Xin et al., 2017), the 3.80 g/L VSS loss was able to generate 5.40 g/L SCOD increase empirically. Thus, it could be speculated that the 5.35 g/L SCOD increase could be attributed reasonably to the 3.80 g/L VSS solubilization by the enzymolysis in this study.

Soluble substance variations during the co-fermentation

It was clear that SCOD increased slightly in the first 2 days from about 7500 to 9000 mg/L and then reduced to about 4200 mg/L finally in fermentation experiment 1 (fed with the mixture of pretreated WAS, CS, and PM) (Fig. 2a). The initial TSS was about 19.25 g/L with 12.38 g/L VSS. Subsequently, the TSS changed to 18.53 g/L with 11.21 g/L VSS when the soluble COD increased to 9000 mg/L on day 2. It could be concluded that the 1.17 g/L VSS reduction caused a 1500 mg/L COD increase approximately according to the relationship of SCOD with VSS discussed above. The soluble COD in fermentation experiment 2 (fed with pretreated WAS and CS) kept similar concentration levels with the fermentation experiment 1 and reduced sharply to nearly 4000 mg/L on day 10. The soluble COD of fermentation experiment 3 (fed with pretreated WAS) increased in the first 2 operational days as well from 5500 to 6500 mg/L and then reduced to 1800 mg/L on day 10.

The soluble protein decreased obviously from 2700 to 1500 mg/L in fermentation test 1 and from 2680 to 1000 mg/L in fermentation test 2 on day 8. The soluble protein reduced gradually from 1000 mg/L to nearly 500 mg/L in fermentation experiment 3 (Fig. 2b). The soluble carbohydrate contents decreased from 1400 to 300 mg/L levels similarly in fermentation experiments 1 and 2. The soluble carbohydrate contents were kept at the levels of 200–300 mg/L in fermentation test 3 (Fig. 2c). The changes of soluble substances could be attributed to the dynamic balance between the feedstock solubilization and consumptions for acidogenesis (Fig. 3a) (Yu et al. 2003).

VFA accumulation, biogas generation, and EEM observations

The VFA accumulation augmented obviously and reached peak values (more than 5100 mg COD/L in fermentation experiment 1 and 4800 mg COD/L in fermentation experiment 2) just within 3–4 fermentation days (Fig. 3a). Moreover, the total VFA content kept higher levels in fermentation experiment 1 with a final concentration of around 3700 mg COD/L ultimately compared to that in fermentation experiment 2. In fermentation experiments 3 and 4, the VFA accumulation levels ranged from 500 to 2000 mg COD/L approximately. It could be confirmed that the CS and PM addition for C/N ratio adjustment not only augmented VFA accumulation quantity obviously but also shortened the retention time of reaching the highest VFA content. The 20/1 was a suitable feedstock C/N ratio for microbial physiology, leading to the greatest hydrolytic enzyme activities (Jia et al. 2013). In terms of the individual VFA, acetate was the prevalent VFA at the early fermentation stage (the first 5 days) with more than 60% percentage in fermentation experiments 1 and 2 (CS and/or PM addition), while the propionate tended to be the dominant VFA at the terminal fermentation stage (the last 3 days) with more than 50% proportion (Fig. 3b, c). However, the acetate and propionate dominated the total VFAs constantly in WAS fermentation processes 3 and 4 (Fig. 3d, e). The fermentation type changes might be attributed to the system pH and ORP variations, both of which played crucial roles in regulating the relative proportion between obligate anaerobe bacteria and facultative anaerobic bacteria in the microbial community during the fermentation process (Su et al. 2016). In addition, the biogas accumulation was collected (data not shown). Compared with the control tests (without CS/PM addition), the cumulative biogas yields reached about 350 mL/g VSS in the co-fermentations of WAS and CS or PM, which were mainly consisted of CO₂ and H₂. The sum volume of CO₂ and H₂ accounted for over 90% of total gas volume, which inferred that the methanogenesis was nearly inhibited in the 10-day-fermentation.

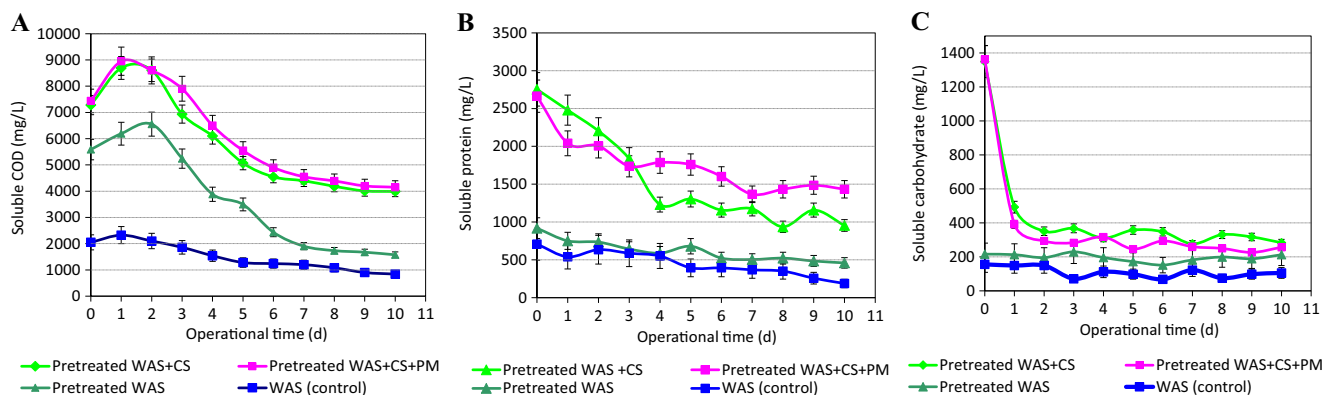


Fig. 2 Soluble organic substance changes in the fermentation/co-fermentation process. **a** Soluble COD. **b** Soluble protein. **c** Soluble carbohydrate

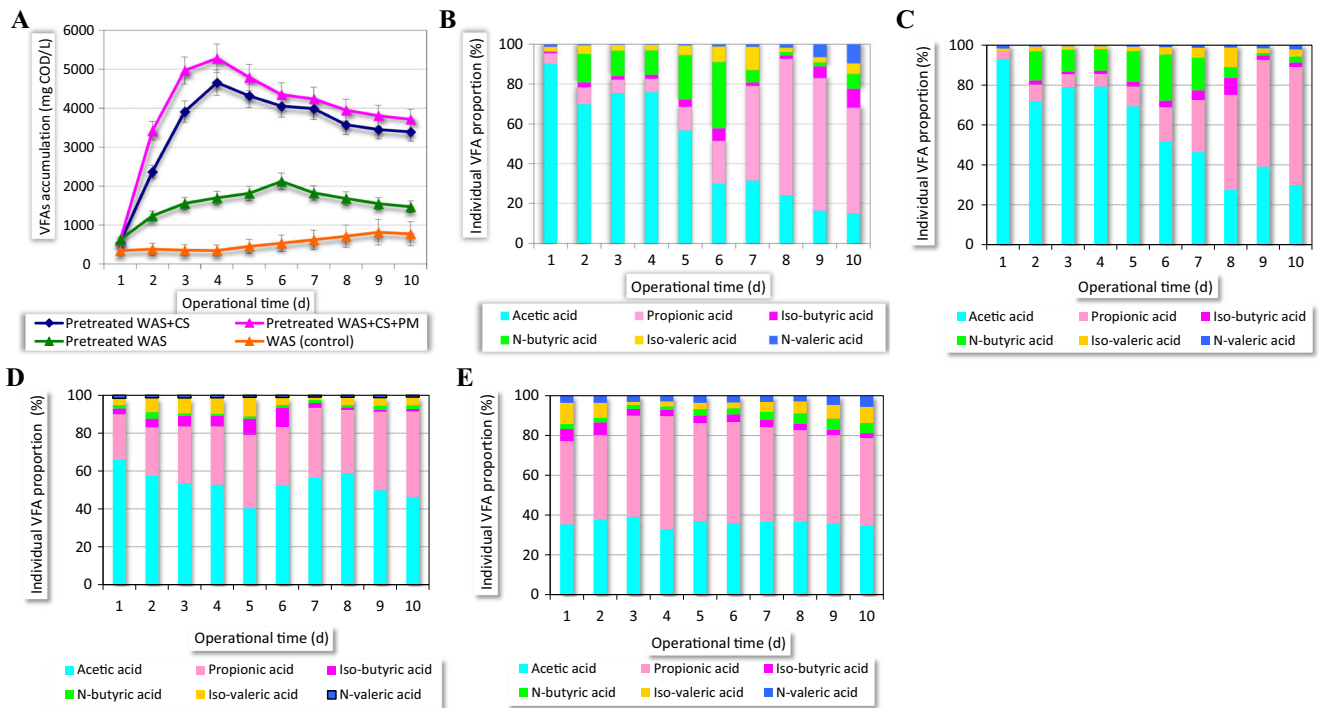


Fig. 3 VFA accumulation and composition in the fermentation/co-fermentation process. **a** Performance of VFAs accumulation. **b–e** Percentage of individual VFA accounting for total VFAs fed with **b** pretreated WAS + CS + PM, **c** pretreated WAS + CS, **d** pretreated WAS, and **e** WAS (control)

The EEM fluorescence spectra depicted the dominant soluble organics in the liquid phase in the fermentation system. In the mixed waste fermentation process (fermentation process 1), three main peaks at Ex/Em 275–280/310–320 nm (labeled as peak 1), 260–275/350–360 nm (peak 2), and 300–310/400–410 nm (peak 3) were observed obviously (Fig. S1). It was obvious that the maximal fluorescence intensities of all peaks emerged on day 3 (Fig. S1B) and then reduced gradually with the fermentation process ongoing (Fig. S1 C–F), which was coincided with the VFA accumulation closely (Fig. 3a). However, just two weak peaks (peaks 1 and 2) appeared in the control fermentation (Fig. S1E–H) with much lower fluorescence intensities compared with those in fermentation process 1. Peak 1 (at Ex/Em 275–280/310–320 nm) and peak 2 (at Ex/Em 260–275/350–360 nm) were related to the protein-like substance, such as tyrosine and tryptophan, while peak 3 (at Ex/Em 300–310/400–410 nm) was associated closely with humic acid-like organics (Chen et al. 2003). The tryptophan protein-like substances were believed to represent the fraction of biodegradable compounds, which were easily used for the energy requirements of acidogenic microorganisms (He et al. 2011).

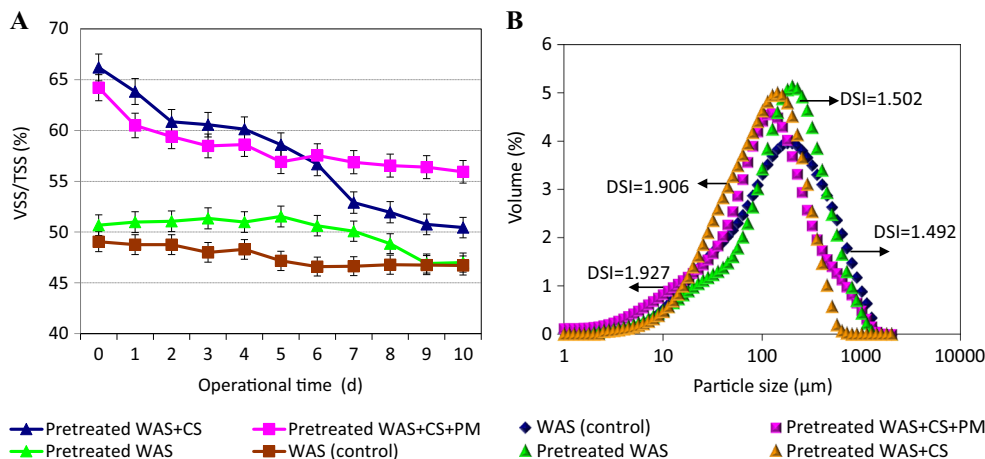
VSS/TSS and particle size variations

The VSS/TSS ratio was used to reflect the biomass conversion efficiency from the solid to liquid phase. It was obvious that the VSS/TSS of mixed wastes decreased clearly from nearly

65 to 55% in fermentation experiment 1 and from 66 to 50% in fermentation experiment 2, respectively (Fig. 4a), while the VSS/TSS decreased slightly from 50 to 46% approximately in the pure pretreated WAS fermentation and control test. It inferred that C/N of 20/1 of feed (by external substances adjustment) favored the hydrolysis performance and improved the biomass transfer efficiency from the solid to liquid during the fermentation process compared to the fermentations with the C/N ratio of 9/1. It was reported that the hydrolysis could be significantly improved with the feedstock C/N ratio of 20/1 due to the most active hydrolytic enzymes (Jia et al. 2013). The high hydrolysis performance of soluble substances (soluble carbohydrate and protein) played positive roles on the great accumulation of VFAs (Fig. 3a).

The morphological property changes of fermentative wastes were associated closely with the filtration trait of fermentation residuals. Figure 4b depicted the particle size variation and DSI changes. It was observed that a relatively wide particle size distribution was displayed in the control fermentation with the lowest DSI of 1.492. The particle size distribution narrowed with the DSI of 1.502 in the pretreated WAS fermentation process. It tended to be further decreased in the mixed-waste fermentation processes with the DSI values of 1.906 in fermentation process 2 and 1.927 in fermentation process 1, respectively. The particle size reduction improved the anaerobic biodegradability performance of the substrate and positively influences the rate of hydrolysis, thereby resulting in a high anaerobic fermentation performance

Fig. 4 Characteristics changes of the fermentative substrates in the fermentation/co-fermentation process. **a** VSS/TSS variations. **b** Particle size distribution changes



(Kondusamy and Kalamdhad 2014). The particle size reducing might be caused by the fact of the deflocculation performance induced by hydrolysis exceeding the protein-aided bioflocculation in the fermentation process, which were two simultaneously occurring and competing effects (Teo and Wong 2014). Moreover, the DSI value of floc size distribution played an important role in increasing specific cake resistance of sludge, where the minimum specific cake resistance occurred at the lowest DSI (Mohamed 2008). High DSI implied the sludge with worse aggregation and high compressibility (Su et al. 2013), which would be beneficial for the further disposal of fermentative residuals. Thus, the CS and PM addition in the co-fermentation not only promoted the VFA accumulation performance by improving the feedstock C/N ratio but also benefitted the further disposal/management of fermentative residuals by favoring the compressibility potential of fermentative wastes.

Microbial community profiles

The T-RFLP profiles on bacterial community of all fermentation processes were depicted in Fig. 5 and Table 3. It was clear that T-RFs of 65 bp (15–30% relative abundance, *Proteiniborus*) and 459 bp (10–15%) ruled the communities from days 1 to 5, while the T-RFs of 149 bp (20–40%), 213 bp (10–30%), and 470 bp (20%) were the main taxa from days 7 to 10 in fermentation process 1 (Fig. 5a). In fermentation process 2, the T-RFs of 556 bp (20%, *Lactobacillus*), 67 bp (20–40%, *Proteiniborus*), and 553 bp (15–20%) occupied the top positions from days 1 to 5 with the T-RFs of 290 bp (10–20%), 293 bp (20%, *Firmicutes*), 220 bp (15%), and 560 bp (10%, *Lactobacillus*) dominating the communities in the residual fermentation period (Fig. 5b). Comparatively, the T-RFs of 458 bp (15–20%), 468 bp (5–25%), 471 bp (10–15%), 218 bp (20%, *Clostridium*), and 558 bp (18%, *Lactobacillus*) were the vital taxa in fermentation process 3 (Fig. 5c). The *Lactobacillus* was associated with the

degradation of proteins and lipids during the fermentation (Jang et al., 2016). The *Clostridium* existed as the minor T-RFs, which was responsible for the degradation of various carbohydrates (Lee et al., 2011). The microbial consortia structure and dynamics were related to system performance stability since microbial community composition variations were often associated with the functional capability changes of communities (Hai et al. 2014). The fact of acetate-type fermentation changing to propionate-type fermentation (operational day 5 was the demarcation point) (Fig. 3b, c) indicated that the fermentation type changes were associated with community dynamics obviously, which might be attributed to the feed composition differences (trophic level changes) (Table 2). The differences of feedstock contributed considerably to microbial community profile changes in waste anaerobic fermentation process. The dynamic balance between the two major domains (bacteria and archaea) was associated closely with the consistency of VFA accumulation (Jang et al. 2016). Thus, it could be confirmed that the CS and PM addition played a vital role on microbial community composition and dynamics in the WAS fermentation process, achieving the highest VFA yield at the feed C/N ratio of 20/1, which was supported by a previous study proposing that the activities of metabolic enzymes for hydrolysis and acidification arriving to the highest at C/N ratio of 20/1 comparing with other C/N ratios (Jia et al. 2013).

Community diversity and evenness

The bacterial community diversity changes in all fermentation processes are depicted in Fig. 6. The diversity of bacterial community increased slightly with the fermentation process ongoing. It was clear that community diversity in fermentations fed with mixed substrates got to be higher (rising from 2.5 to 3.0 in the bacterial community) than those without external carbon source addition. Diversity increase was related to system performance stability (function) positively (Loreau

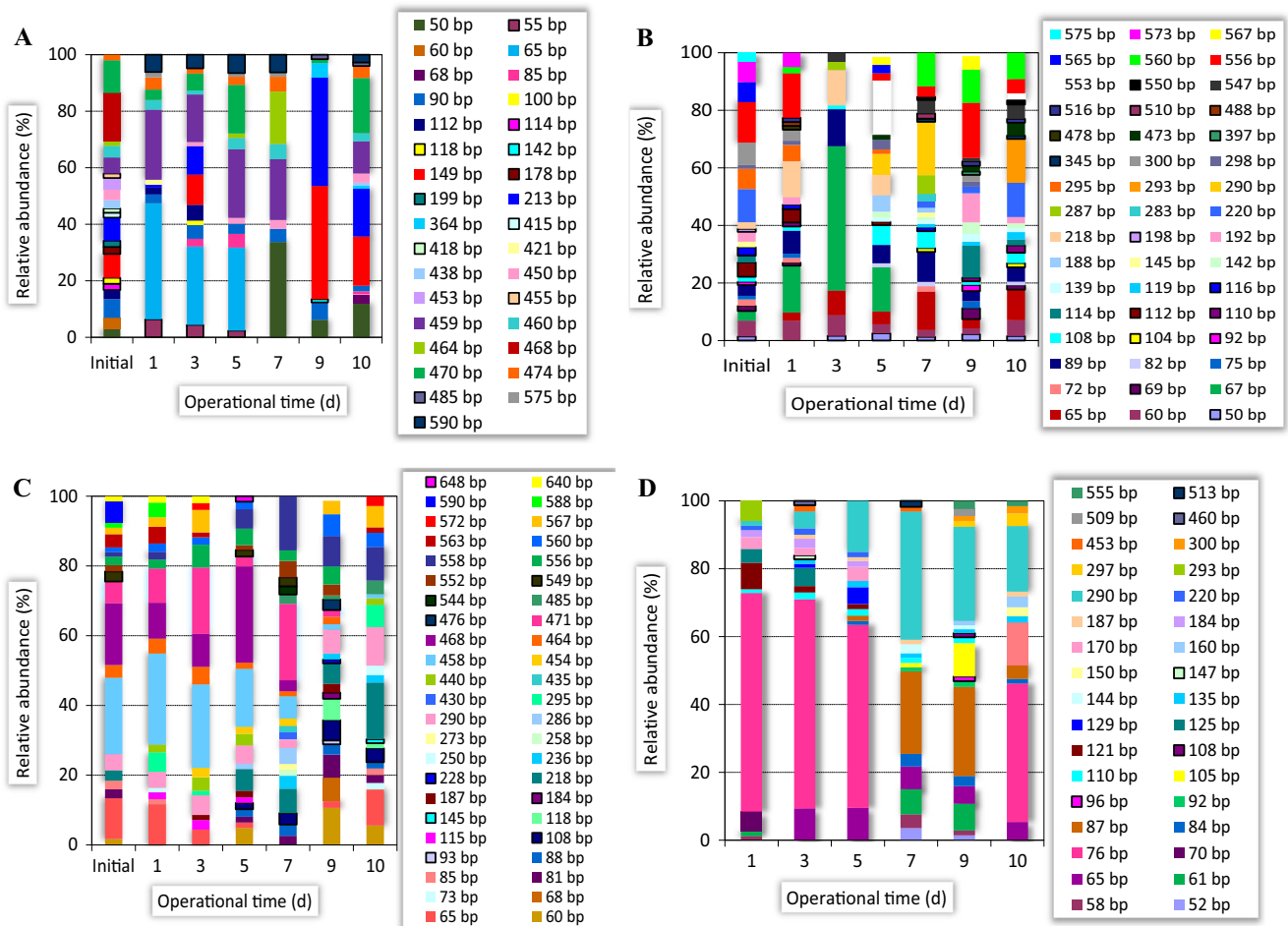


Fig. 5 T-RFLP profiles for depicting the bacterial community dynamics in the fermentation/co-fermentation process. **a** Pretreated WAS + CS + PM. **b** Pretreated WAS + CS **c** Pretreated WAS. **d** Fresh WAS

et al. 2001). Little fluctuations of diversity emerged at the initial fermentation process might be associated with the unstable community structure without forming completely

(unbalance between the domain of bacterial and archaeal), which caused relatively low VFA production efficiency (Fig. 3a). It was obvious that the addition of CS and PM favored the community diversity rising and further improved the acidogenesis process performance in WAS fermentation process.

Table 3 The main taxonomic contributors corresponding to the T-RFs in the fermentation/co-fermentation process

T-RFs	Main taxonomic contributors
56 bp	<i>Olsenella</i>
62 bp	<i>Anaerotruncus</i>
67 bp	<i>Proteiniborus</i>
138 bp	<i>Pelotomaculum</i>
155 bp	<i>Pelotomaculum</i>
175 bp	<i>Gallicola</i>
178 bp	<i>Lactobacillus</i>
198 bp	<i>Synergistaceae</i>
280 bp	<i>Clostridium IV</i>
208 bp	<i>Clostridium</i>
296 bp	<i>Firmicutes</i>
361 bp	<i>Bacteroidales</i>
516 bp	<i>Clostridiaceae</i>
562 bp	<i>Lactobacillus</i>

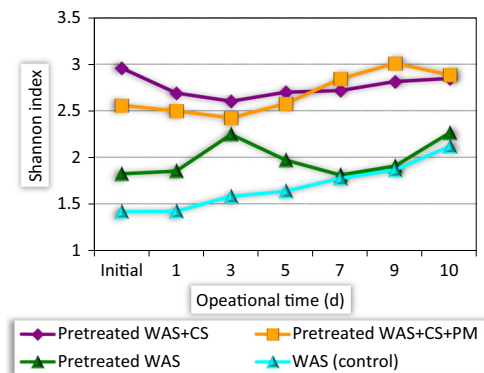


Fig. 6 Bacterial community diversity shifts in the fermentation/co-fermentation process

The PL curve was used to evaluate the bacterial community distributive evenness figuratively. Feedstock differences played vital roles on bacterial community evenness (Fig. 7) in fermentation processes. At the fermentation prophase (day 3), all PL curves were nearly coincided, which inferred that the divergences of bacterial community evenness appeared to be slight and indistinctive (Fig. 7a). However, the PL curve got far from the theoretical perfect line (45° diagonal line) gradually with the fermentation process ongoing by the CS and PM addition, which indicated that the bacterial community equitability got to be uneven dramatically at the fermentation terminal stage (Fig. 7b). Based on the Pareto's law, the value of the vertical axis was in accordance with 20% abscissa axis, being used to interpret the PL curves (Wittebolle et al. 2008). The uneven community distribution contributed to the system performance stability within a system (Hillebrand et al. 2008). Thus, it could be speculated that the CS and PM addition changed the bacterial community arrangement with forming uneven community distribution in the fermentation system, which inferred that a relatively uneven distribution of bacterial community contributed to the constant VFA accumulation positively.

Correlation of microbial community composition with environmental variables

Detrended correspondence analysis (DCA) by Canoco 4.5 software inferred that the correlations of environmental variables (OLR, pH and ORP in this study) with bacterial community compositions were depicted properly by the redundancy analysis (RDA). In fermentation process 1, RDA plots based on the correlations of impact factors (Fig. S2) with T-RFs (resulted from T-RFLP analysis) were performed by Canoco 4.5 software in Fig. 8. Monte Carlo permutation tests confirmed the distributions were non-random ($P < 0.05$). The vectors of pH and ORP played positive roles on bacterial

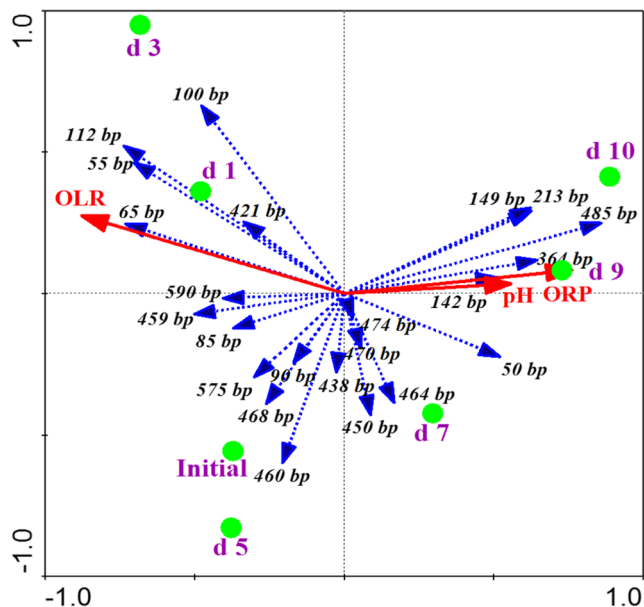
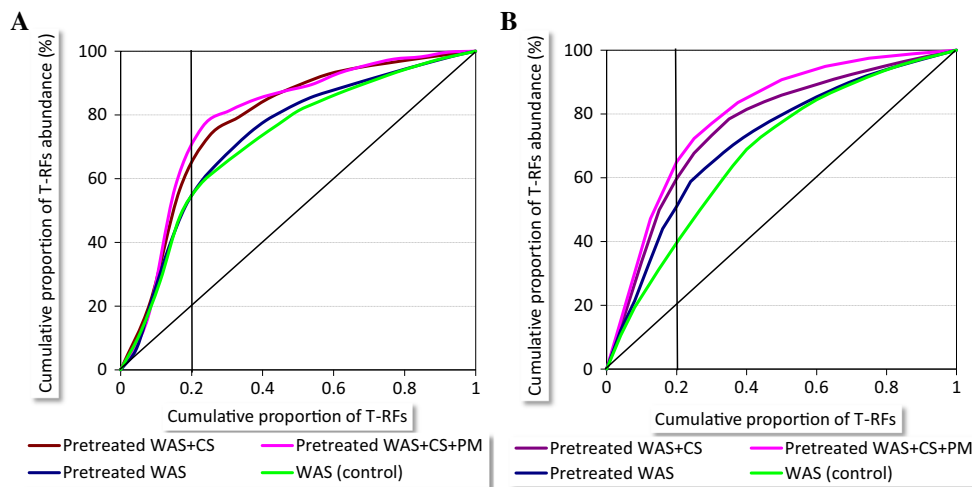


Fig. 8 Correlations of bacterial community composition with environmental variables in the co-fermentation process fed with pretreated WAS + CS + PM. The environmental variables (pH, OLR, and ORP) are shown as red vectors in the plot. The brown arrows stand for T-RFs. The bright green dots stand for the community of each sample. The correlation coefficients of bacterial spec axis 1 and axis 2 with ORP (environmental variable 1) were 0.627 and 0.045, with pH (environmental variable 2) 0.459 and 0.019, and with OLR (environmental variable 3) -0.722 and 0.816, respectively. The species-environment correlations on axis 1 and axis 2 were 0.859 and 0.149

communities on days 7, 9, and 10 (main T-RFs of 149, 213, 485, and 364 bp), which located in the first quadrant. In contrast, the OLR had a negative impact on microbial communities (on days 1 and 3) at the prophase of the fermentation process, which located in the second quadrant containing the main T-RFs of 100, 112, 55, 421, and 65 bp. Besides, the samples from the first 5 fermentation days and the residual operational days (days 7, 9, and 10) were distinctly separated by axis 2 completely. It was proposed that adjustments of

Fig. 7 Pareto-Lorenz curves derived from T-RFLP profiles for evaluating bacterial community distributive evenness in the co-fermentation process (WAS + CS + PM). **a** Operational day 3. **b** Operational day 10



OLR, pH, and ORP could change the fermentation type in the acidogenesis process (Chen et al. 2015), which were responsible for the individual VFA proportion variations as well (Fig. 3b–e).

Furthermore, the pH increase (reached 7.7 ultimately) might be related to the alkaline pretreatment of CS and PM (Fig. S2A). The ORP increased gradually (rising from -400 mV to -380 mV) in the first six operational days in fermentation process 1 (Fig. S2B), which played a positive role on VFA accumulation, supported by Su et al. using citrus waste as external carbohydrates for boosting sludge fermentation performance (Su et al. 2016). The OLR augmented in the first 2 days and then reduced clearly till the end of the fermentation (Fig. S2C). Some researchers proposed that pH played a more significant role than ORP in regulating fermentation type in the acidogenesis (Chen et al. 2015). However, the ORP also played vital roles on the anaerobic fermentation by regulating the proportion between obligate anaerobe bacteria and facultative anaerobic bacteria in sludge fermentation (Su et al. 2016). Indeed, the effects of pH or ORP on the fermentation process were synergetic rather than isolated and independent (Fig. S2). Song et al. proposed that the distinction of bacteria groups influenced by pH value resulted in the difference of coherence, which was related to the secretion of extracellular polysaccharide (Song et al. 2011). This phenomenon had an important impact on ORP variations in fermentation system. Thus, the ORP, pH, and OLR had synergetic effects on fermentation performance and microbial community dynamics inherently (Figs. 6 and 7), supported by a previous study (Chen et al. 2015). The VFA generation relied considerably on the proper operations based on the relationship between bacterial community composition and impact factors (ORP, pH, and OLR) for optimizing the fermentation process. It could be recognized that CS and PM addition regulated the ORP within the range of -380 to -320 mV, which facilitated VFA accumulation with the pH of 6.5–7.5 in this study.

Conclusions

The results above gave a feasible way to enhance VFA generation by adding corn stalk and pig manure to adjust C/N ratio to boost VFA accumulation obviously from WAS. The VFA accumulation was achieved significantly to over 5000 mg COD/L just within 4–5 days in the co-fermentation with the regulated C/N ratio of 20/1. Meanwhile, the CS and PM addition improved the compressibility of fermentation-mixed residuals in the co-fermentation. Moreover, the external carbon addition conducted to bacterial consortia diversity rising and poor population evenness, which improved the acidification performance. Finally, the optimizations of OLR at the initial fermentation stage, pH (6.5–7.5), and ORP (from -380

to -320 mV) at the terminal fermentation stage were favorable to VFA accumulation during the co-fermentation operation.

Funding information This research was supported financially by the Program of International S&T Cooperation (2016YFE0123400), National Natural Science Foundation of China (No.51778179), China Scholarship Council (CSC, 201606120198), State Key Laboratory of Urban Water Resource and Environment (Harbin Institute of Technology) (No. 2016TS02), and Heilongjiang Province Science Foundation for General Program (E201427).

References

- Alqaralleh RM (2016) Thermophilic and hyper-thermophilic co-digestion of waste activated sludge and fat, oil and grease: evaluating and modeling methane production. *J Environ Manag* 183(Pt 3):551–561. <https://doi.org/10.1016/j.jenvman.2016.09.003>
- APHA (1998) Standard methods for the examination of water and wastewater, 20th edn. American Public Health Association, Washington, DC, USA
- Barber WPF (2016) Thermal hydrolysis for sewage treatment: a critical review. *Water Res* 104:53–71. <https://doi.org/10.1016/j.watres.2016.07.069>
- Bruce ER, Perry LM (2001) Environmental biotechnology: principles and applications. McGrawHill, New York, p 400
- Chen W, Weatherhoff P, Leenheer JA, Booksh K (2003) Fluorescence excitation-emission matrix regional integration to quantify spectra for dissolved organic matter. *Environ Sci Technol* 37(24):5701–5710. <https://doi.org/10.1021/es034354c>
- Chen X, Yuan HR, Zou DX, Liu YP, Zhu BN, Chufu A, Jaffar M, Li XJ (2015) Improving biomethane yield by controlling fermentation type of acidogenic phase in two-phase anaerobic co-digestion of food waste and rice straw. *Chem Eng J* 273:254–260. <https://doi.org/10.1016/j.cej.2015.03.067>
- Chen YG, Luo JY, Yan YY, Feng LY (2013) Enhanced production of short-chain fatty acid by co-fermentation of waste activated sludge and kitchen waste under alkaline conditions and its application to microbial fuel cells. *Appl Energy* 102:1197–1204. <https://doi.org/10.1016/j.apenergy.2012.06.056>
- Dai XH, Li XS, Zhang D, Chen YG, Dai LL (2016) Simultaneous enhancement of methane production and methane content in biogas from waste activated sludge and perennial ryegrass anaerobic co-digestion: the effects of pH and C/N ratio. *Bioresour Technol* 216:323–330. <https://doi.org/10.1016/j.biortech.2016.05.100>
- Feng LY, Chen YG, Zheng X (2009) Enhancement of waste activated sludge protein conversion and volatile fatty acids accumulation during waste activated sludge anaerobic fermentation by carbohydrate substrate addition: the effect of pH. *Environ Sci Technol* 43(12):4373–4380. <https://doi.org/10.1021/es8037142>
- Guo XH, Wang C, Sun FQ, Zhu WJ, WX W (2014) A comparison of microbial characteristics between the thermophilic and mesophilic anaerobic digesters exposed to elevated food waste loadings. *Bioresour Technol* 152:420–428. <https://doi.org/10.1016/j.biortech.2013.11.012>
- Hai R, Wang YL, Wang XH, Li Y, ZZ D (2014) Bacterial community dynamics and taxa-time relationships within two activated sludge bioreactors. *PLoS One* 9:1–8
- He XS, Xi BD, Wei ZM, Jiang YH, Yang Y, An D, Cao JL, Liu HL (2011) Fluorescence excitation–emission matrix spectroscopy with regional integration analysis for characterizing composition and transformation of dissolved organic matter in landfill leachates. *J Hazard*

- Mater 190(1-3):293–299. <https://doi.org/10.1016/j.jhazmat.2011.03.047>
- Hillebrand H, Bennett DM, Cadotte MW (2008) Consequences of dominance: a review of evenness effects on local and regional ecosystem processes. *Ecology* 89(6):1510–1520. <https://doi.org/10.1890/07-1053.1>
- Jang HM, Ha JH, Kim M-S, Kim J-O, Kim YM, Park JM (2016) Effect of increased load of high-strength food wastewater in thermophilic and mesophilic anaerobic co-digestion of waste activated sludge on bacterial community structure. *Water Res* 99:140–148. <https://doi.org/10.1016/j.watres.2016.04.051>
- Jia ST, Dai XH, Zhang D, Dai LL, Wang RC, Zhao JF (2013) Improved bioproduction of short-chain fatty acids from waste activated sludge by perennial ryegrass addition. *Water Res* 47(13):4576–4584. <https://doi.org/10.1016/j.watres.2013.05.012>
- Jiang D, Zhuang D, Fu J, Huang Y, Wen K (2012) Bioenergy potential from crop residues in China: availability and distribution. *Renew Sust Energ Rev* 16(3):1377–1382. <https://doi.org/10.1016/j.rser.2011.12.012>
- Jiang Y, Chen YG, Zheng X (2009) Efficient polyhydroxyalkanoates production from a waste-activated sludge alkaline fermentation liquid by activated sludge submitted to the aerobic feeding and discharge process. *Environ Sci Technol* 43(20):7734–7741. <https://doi.org/10.1021/es9014458>
- Kondusamy D, Kalamdhad AS (2014) Pre-treatment and anaerobic digestion of food waste for high rate methane production—a review. *J Environ Chem Eng* 2(3):1821–1830. <https://doi.org/10.1016/j.jece.2014.07.024>
- Lee DJ, Show KY, Su A (2011) Dark fermentation on biohydrogen production: pure culture. *Bioresour Technol* 102(18):8393–8402. <https://doi.org/10.1016/j.biortech.2011.03.041>
- Li X, Chen H, LF H, Yu L, Chen YG, GW G (2011) Pilot-scale waste activated sludge alkaline fermentation, fermentation liquid separation, and application of fermentation liquid to improve biological nutrient removal. *Environ Sci Technol* 45(5):1834–1839. <https://doi.org/10.1021/es1031882>
- Li YM, Wang J, Zhang A, Wang L (2015) Enhancing the quantity and quality of short-chain fatty acids production from waste activated sludge using CaO₂ as an additive. *Water Res* 83:84–93. <https://doi.org/10.1016/j.watres.2015.06.021>
- Lo KV, Liao PH, Srinivasan A (2016) Continuous-flow microwave enhanced oxidation process for treating sewage sludge. *Can J Chem Eng* 94(7):1285–1294. <https://doi.org/10.1002/cjce.22510>
- Loreau M, Naeem S, Inchausti P, Bengtsson J, Grime JP (2001) Biodiversity and ecosystem functioning: current knowledge and future challenges. *Science* 294(5543):804–808. <https://doi.org/10.1126/science.1064088>
- Lu JB, Zhu L, GL H, JG W (2010) Integrating animal manure-based bioenergy production with invasive species control: a case study at Tongren pig farm in China. *Biomass Bioenergy* 34:821–827
- Luo JY, Feng LY, Zhang W, Li X, Chen H, Wang DB, Chen YG (2014) Improved production of short-chain fatty acids from waste activated sludge driven by carbohydrate addition in continuous-flow reactors: influence of SRT and temperature. *Appl Energy* 113:51–58. <https://doi.org/10.1016/j.apenergy.2013.07.006>
- Mahdad F, Younesi H, Bahramifar N, Hadavifar M (2016) Optimization of Fenton and photo-Fenton-based advanced oxidation processes for post-treatment of composting leachate of municipal solid waste by an activated sludge process. *KSCE J Civ Eng* 20(6):2177–2188. <https://doi.org/10.1007/s12205-015-1045-1>
- Marzorati M, Wittebolle L, Boon N, Daffonchio D, Verstraete W (2008) How to get more out of molecular fingerprints: practical tools for microbial ecology. *Environ Microbiol* 10(6):1571–1581. <https://doi.org/10.1111/j.1462-2920.2008.01572.x>
- Michel D, Gilles KA, Hamilton JK, Rebers PA, Smith F (1956) Colorimetric method for determination of sugars and related substances. *Anal Chem* 28:350–356
- Mohamed B (2008) Filtration characteristics of a mineral mud with regard to turbulent shearing. *J Membr Sci* 320(1–2):533–540
- Morowitz MJ, Deneff VJ, Costello EK, Thomas BC, Poroyko V, Relman DA, Banfield JF (2011) Strain-resolved community genomic analysis of gut microbial colonization in a premature infant. *Proc Natl Acad Sci* 108(3):1128–1133. <https://doi.org/10.1073/pnas.1010992108>
- Nielsen HB, Angelidaki I (2008) Strategies for optimizing recovery of the biogas process following ammonia inhibition. *Bioresour Technol* 99(17):7995–8001. <https://doi.org/10.1016/j.biortech.2008.03.049>
- Parmar N, Singh A, Ward OP (2001) Enzyme treatment to reduce solids and improve settling of sewage sludge. *J Ind Microbiol Biotechnol* 26(6):383–386. <https://doi.org/10.1038/sj.jim.7000150>
- Saikaly PE, Strood PG, Oerther DB (2005) Use of 16S rRNA gene terminal restriction fragment analysis to assess the impact of solids retention time on the bacterial diversity of activated sludge. *Appl Environ Microbiol* 71(10):5814–5822. <https://doi.org/10.1128/AEM.71.10.5814-5822.2005>
- Salsabil MR, Prorot A, Casellas M, Dagot C (2009) Pre-treatment of activated sludge: effect of sonication on aerobic and anaerobic digestibility. *Chem Eng J* 148(2-3):327–335. <https://doi.org/10.1016/j.cej.2008.09.003>
- Song JX, An D, Ren NQ, Zhang YM, Chen Y (2011) Effects of pH and ORP on microbial ecology and kinetics for hydrogen production in continuously dark fermentation. *Bioresour Technol* 102(23):10875–10880. <https://doi.org/10.1016/j.biortech.2011.09.024>
- Su HF, Tan FR, YJ X (2016) Enhancement of biogas and methanization of citrus waste via biodegradation pretreatment and subsequent optimized fermentation. *Fuel* 181:843–851
- Su XY, Tian Y, Li H, Wang CN (2013) New insights into membrane fouling based on characterization of cake sludge and bulk sludge: an especial attention to sludge aggregation. *Bioresour Technol* 128:586–592
- Teo CW, Wong PCY (2014) Enzyme augmentation of an anaerobic membrane bioreactor treating sewage containing organic particulates. *Water Res* 48:335–344. <https://doi.org/10.1016/j.watres.2013.09.041>
- Turner S, Pryer KM, Miao VPW, Palmer JD (1999) Investigating deep phylogenetic relationships among cyanobacteria and plastids by small subunit rRNA sequence analysis. *J Eukaryot Microbiol* 46(4):327–338. <https://doi.org/10.1111/j.1550-7408.1999.tb04612.x>
- Wittebolle L, Marzorati M, Clement L, Balloi A, Daffonchio D (2009) Initial community evenness favours functionality under selective stress. *Nature* 458(7238):623–626. <https://doi.org/10.1038/nature07840>
- Wittebolle L, Vervaeren H, Verstraete W, Boon N (2008) Quantifying community dynamics of Nitrifiers in functionally stable reactors. *Appl Environ Microbiol* 74(1):286–293. <https://doi.org/10.1128/AEM.01006-07>
- Xin XD, He JG, Feng JH, Li L, Wen ZD, Hu Q, Qiu W, Zhang J (2016) Solubilization augmentation and bacterial community responses triggered by co-digestion of a hydrolytic enzymes blend for facilitating waste activated sludge hydrolysis process. *Chem Eng J* 284:979–988. <https://doi.org/10.1016/j.cej.2015.09.060>
- Xin XD, He JG, Li L, Qiu W (2017) Enzymes catalyzing pre-hydrolysis facilitated the anaerobic fermentation of waste activated sludge with acidogenic and microbiological perspectives. *Bioresour Technol* 250:69–78. <https://doi.org/10.1016/j.biortech.2017.09.211>
- Yan YY, Feng LY, Zhang CJ, Wisniewski C, Zhou Q (2010) Ultrasonic enhancement of waste activated sludge hydrolysis and volatile fatty acids accumulation at pH 10.0. *Water Res* 44(11):3329–3336. <https://doi.org/10.1016/j.watres.2010.03.015>

- Yang G, Zhang GM, Wang HC (2015) Current state of sludge production, management, treatment and disposal in China. *Water Res* 78:60–73. <https://doi.org/10.1016/j.watres.2015.04.002>
- Yang Q, Luo K, Li XM, Wang DB, Zheng W, Zeng GM, Liu JJ (2010) Enhanced efficiency of biological excess sludge hydrolysis under anaerobic digestion by additional enzymes. *Bioresour Technol* 101(9):2924–2930. <https://doi.org/10.1016/j.biortech.2009.11.012>
- Yu H, Zheng X, Hu Z, Gu G (2003) High-rate anaerobic hydrolysis and acidogenesis of sewage sludge in a modified upflow reactor. *Water Sci Technol* 48(4):69–75
- Yu SY, Zhang GM, Li JZ, Zhao ZW, Kang XR (2013) Effect of endogenous hydrolytic enzymes pretreatment on the anaerobic digestion of sludge. *Bioresour Technol* 146:758–761
- Zheng HZ, Li DW, Stanislaus MS, Zhang N, Zhu Q, XH H, Yang YN (2015) Development of a bio-zeolite fixed-bed bioreactor for mitigating ammonia inhibition of anaerobic digestion with extremely high ammonium concentration livestock waste. *Chem Eng J* 280: 106–114. <https://doi.org/10.1016/j.cej.2015.06.024>
- Ziels RM, Karlsson A, Beck DAC, Ejlertsson J, Yekta SS, Bjorn A, Stensel HD, Svensson BH (2016) Microbial community adaptation influences long-chain fatty acid conversion during anaerobic codigestion of fats, oils, and grease with municipal sludge. *Water Res* 103:372–382. <https://doi.org/10.1016/j.watres.2016.07.043>